

# protein phosphatase 2A structural/scaffold subunit A, alpha isoform (PPP2R1A) : Time behavioural study of 3rd order combinations in WNT3A stimulated HEK 293 cells

shriprakash sinha

*Independent Researcher; Orcid ID : [orcid.org/0000-0001-7027-5788](https://orcid.org/0000-0001-7027-5788)*

*Address : 104-Madhurisha Heights Phase I, Risali, Bhilai-490006, India*

*Corresponding author email : [sinha.shriprakash@yandex.com](mailto:sinha.shriprakash@yandex.com)*

---

## Abstract

PPP2R1A forms a component of the PP2A holoenzyme complex. PPP2R1A is the predominant PP2A scaffold A-subunit that is required for functional PP2A complex formation and PPP2R1A depletion results in comprehensive PP2A complex inhibition. Gujral and MacBeath [1] provides a quantitative, and dynamic study of WNT3A-mediated stimulation of HEK 293 cells, where they record time based expression profiles of several response genes which correlated significantly with proliferation and migration. By monitoring the dynamics of gene expression using self-organizing maps, they identified clusters of genes that exhibit similar expression dynamics and uncovered previously unrecognized positive and negative feedback loops. However, their study depicts/uses singular measurements of individual gene expression at different time snapshots/points to infer the system wide analysis of the pathway. At any particular time point, it is often the case that genes are working synergistically in combinations, even though their expression measurements are singular in nature. Here, I • enumerate and rank all 2415 PPP2R1A related 3rd order combinations in a forest of  ${}^{71}C_3$  combinations using four different sensitivity methods; • show the conserved rankings for PPP2R1A-X-X combinations, which point to existence of biological synergy of some of these combinations across the different sensitivity methods; and • study the behaviour of some of these combinations related to WNT3A response genes that are ranked by the machine learning search engine (Sinha [2]) in time. Patterns of combinations emerge, some of which have been tested in wet lab, while others require further wet lab analysis.

**Keywords:** Sensitivity analysis, Support vector ranking, Hilbert Schmidt Independence Criterion indices (HSIC) and Sobol indices, WNT3A

---

---

<sup>☆</sup>Time behavioural study of 3-odr PPP2R1A comb. in WNT3A stimulated cells

<sup>1</sup>Aspects of unpublished work were presented in a poster session at Cell Symposia: Technology. Biology. Data Science, 9-11 October 2016, Berkeley, California, USA.

## 1. Significance

Sinha [2] recently demonstrated the use of machine learning based search engine to rank/reveal gene combinations at 2nd order for the time series data by Gujral and MacBeath [1] and showed how it is possible to locate combinations of priority that might be working synergistically, using sensitivity methods and powerful support vector ranking algorithm. However, the problem explodes combinatorially with even a small set of 71 recorded genes in the study by Gujral and MacBeath [1], when one steps to explore 3rd order combinations. With the total number of  ${}^{71}C_3$  (= 57155) combinations, it becomes nearly impossible for any biologist to study the system wide dynamics of any pathway. Also, the amount of time usually needed to search for and test a combination is far more than the search down by the machine learning based search engine. Here, I extend the research work by Sinha [2] to conduct a behavioral study of 3rd order PPP2R1A related combinations using individual gene expressions measured in time, in WNT3A stimulated HEK 293 cells.

## 2. Introduction

The details of the machine learning based search engine has been recently published in Sinha [2] and deployed to explore the 2nd order combinations of genes in the data set provided by Gujral and MacBeath [1]. Nevertheless, here, I point to the fundamentals of the published work for completeness.

### 2.1. A combinatorial problem

Sensitivity analysis plays a major role in computing the strength of the influence of involved factors in any phenomena under investigation. When applied to expression profiles of various intra/extracellular factors that form an integral part of a signaling pathway, the variance and density based analysis yields a range of sensitivity indices for individual as well as various combinations of factors. These combinations denote the higher order interactions among the involved factors. Computation of higher order interactions is often time consuming but it gives a chance to explore the various combinations that might be of interest in the working mechanism of the pathway. For example, in a range of fourth order combinations among the various factors of the Wnt pathway, it would be easy to assess the influence of the destruction complex formed by APC, AXIN, CSKI and GSK3 interaction. But the effect of these combinations vary over time as measurements of fold changes and deviations in fold changes vary. So it is imperative to know how an interaction or a combination of the involved factors behave in time and Sinha [2] develops a procedure to track the behaviour by exploiting the influences of these involved factors.

### 2.2. A possible solution

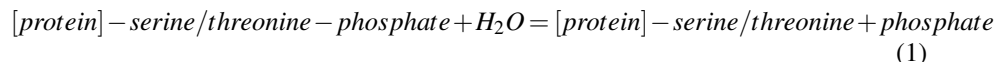
In this work, after estimating the individual effects of factors for a higher order combination, the individual indices are considered as discriminative features. A combination,

then, is a feature set in higher order ( $\geq 2$ , i.e. multivariate). With an excessively large number of factors involved in the pathway, it is difficult to search for important combinations in a wide search space over different orders. Exploiting the analogy with the issues of prioritizing webpages using ranking algorithms, for a particular order, a full set of combinations of interactions can then be prioritized based on these features using a powerful ranking algorithm via support vectors Joachims [3]. Recording the changing rankings of the combinations over time reveals how higher order interactions behave within the pathway and when an intervention might be necessary to influence the interaction within the pathway.

### 2.3. protein phosphatase 2A structural/scaffold subunit A, alpha isoform (PPP2R1A)

Protein phosphorylation is a reversible protein posttranslational modification (PTM). Phosphorylation involves the transfer of phosphate groups from ATP to the enzyme, the energy for which comes from hydrolysing ATP into ADP or AMP. Protein kinases (PKs) are the effectors of phosphorylation and catalyse the transfer of a  $\gamma$ -phosphate from ATP to specific amino acids on proteins. Proteins are phosphorylated predominantly on Ser, Thr and Tyr residues. In contrast, protein phosphatases (PPs) are the primary effectors of dephosphorylation and can be grouped into three main classes based on sequence, structure and catalytic function. Dephosphorylation releases phosphates into solution as free ions, because attaching them back to ATP would require energy input.

PP2A holoenzyme complex comprises a scaffolding (A), regulatory (B), and catalytic (C) subunit, with protein phosphatase 2A, catalytic subunit, alpha isoform (PPP2CA) being the principal catalytic subunit. There are two isoforms of the catalytic (PPP2CA aka  $C\alpha$  and PPP2CB aka  $C\beta$ ), two isoforms of the scaffold A subunit (PPP2R1A aka  $A\alpha$  and PPP2R1B aka  $A\beta$ ) and at least 17 different B subunit proteins that are members of predominantly of three families identified as B family (aka B55; gene symbol PPP2R2), B' family (aka B56; gene symbol PPP2R5) and B'' family (aka PR72/130; gene symbol PPP2R3); and Ruvolo [4] tabulate a few of them and provide references for them. Shi [5] studied the mechanism through structure of the serine/threonine phosphatases. The enzyme protein serine/threonine phosphatase acts upon phosphorylated serine/threonine residues as follows (from Wikipedia contributors [6]) :



In their review, Seshacharyulu et al. [7] focus on the structural complexity of serine/threonine phosphatase PP2A and summarize its expression pattern in cancer while discussing about the PP2A interacting and regulatory proteins and substrates. Finally, they also review the mouse models developed to understand the biological role of PP2A subunits in an in vivo model system. Further, Reinhout and Janssens [8] summarize current knowledge on physiologic functions of PP2A in germ cell maturation, tumor suppression, metabolic regulation, embryonic development, and homeostasis of adult brain, liver, heart, immune system, lung, kidney, intestine, skin, eye and bone, all of which were retrieved from in vivo studies using PP2A transgenic, knockout or knockin

mice.

Hemmings et al. [9] purified Protein phosphatase 2A (polycation-stimulated protein phosphatase L), from porcine kidney and skeletal muscle. Via reverse-phase HPLC, they separated the 36-kDa catalytic and the 65-kDa putative regulatory (hereafter termed PR65) subunits of protein phosphatase 2A2. Molecular cloning showed that two distinct mRNAs (termed  $\alpha$  (PP2A-Aalpha) and  $\beta$  (PP2A-Abeta)) encoded the PR65 subunit. The cDNA encoding the  $\alpha$ -isotype spanned 2.2 kilobases (kb) and contained an open reading frame of 1767 bases predicting a protein of 65 kDa, while the cDNAs encoding the  $\beta$ -isotype contained an open reading frame of size similar to that of  $\alpha$ -form but lacked an initiator ATG. Further, Zhou et al. [10] generated A $\beta$ -specific antibodies and determined the cell cycle expression, subcellular distribution, and metabolic stability of A $\beta$  in comparison with A $\beta$ .

I present 3rd order combinations of PPP2R1A with other genes, that the machine learning based search engine points to, as possible synergistic combinations that might be working in time.

### 3. Methods

Please refer to sections of Sinha [2] for methods, design of study and analysis of data for 2nd order combinations. The same method and design of study is used to generate results for 3rd order combinations presented in this study.

### 4. Time series data

Gujral and MacBeath [1] present a set of 71 WNT-related gene expression values for 6 different time points over a range of 24-hour period using qPCR. The changes represent the fold-change in the expression levels of genes in 200 ng/mL WNT3A-stimulated HEK 293 cells in time relative to their levels in unstimulated, serum-starved cells at 0-hour. Gujral and MacBeath [1] state that qPCR data are the means of three biological replicates. Only genes whose mean transcript levels changed by more than two-fold at one or more time points during the 24-hour time course were considered significant. Positive (negative) numbers represent up (down) -regulation. We have already covered the issues related to these data sets in detail in Sinha [11]. Readers are requested to go through them in the pointed reference. The tools of study which are used here have been published in another foundational work in Sinha [11].

### 5. Design of experiment

#### 5.1. Pipeline for time series data

For the case of time series data, interactions among the contributing factors are studied by comparing triplets of fold-changes at single time points. The procedure begins with the generation of distribution around measurements at single time points with added noise is done to estimate the indices. A distribution is generated for the fold changes

at single time points. Then for every gene, there is a vector of values representing fold changes as well as deviations in fold changes for different time points and durations between time points, respectively. Next a listing of all  $C_k^n$  combinations for  $k$  number of genes from a total of  $n$  genes is generated.  $k$  is  $\geq 2$  and  $\leq (n - 1)$ . Each of the combination of order  $k$  represents a unique set of interaction between the involved genetic factors. After this, the datasets are combined in a specified format which go as input as per the requirement of a particular sensitivity analysis method. Thus for each  $p^{th}$  combination in  $C_k^n$  combinations, the dataset is prepared in the required format from the distributions for two separate cases which have been discussed above. (See .R code in mainScript-1-1.R). After the data has been transformed, vectorized programming is employed for density based sensitivity analysis and looping is employed for variance based sensitivity analysis to compute the required sensitivity indices for each of the  $p$  combinations. This procedure is done for different kinds of sensitivity analysis methods.

After the above sensitivity indices have been stored for each of the  $p^{th}$  combination, the next step in the design of experiment is conducted. Since there is only one recording of sensitivity index per combination, each combination forms a training example which is allotted a training index and the sensitivity indices of the individual genetic factors form the training example. Thus there are  $C_k^n$  training examples for  $k^{th}$  order interaction. Using this training set  $SVM_{learn}^{Rank}$  Joachims [3] is used to generate a model on default value  $C$  value of 20. In the current experiment on toy model  $C$  value has not been tuned. The training set helps in the generation of the model as the different gene combinations are numbered in order which are used as rank indices. The model is then used to generate score on the observations in the testing set using the  $SVM_{classify}^{Rank}$  Joachims [3]. Note that due to availability of only one example per combination, after the model has been built, the same training data is used as test data to generate the scores. This procedure is executed for each and every sensitivity analysis method. This is followed by sorting of these scores along with the rank indices (i.e the training indices) already assigned to the gene combinations. The end result is a sorted order of the gene combinations based on the ranking score learned by the  $SVM^{Rank}$  algorithm. Finally, this entire procedure is computed for sensitivity indices generated for each and every fold change at time point and deviations in fold change at different durations. Observing the changing rank of a particular combination at different times and different time periods will reveal how a combination is behaving.

Note that the following is the order in which the files should be executed in R, in order, for obtaining the desired results (Note that the code will not be explained here) - • use source("mainScript-1-1.R") with arguments for Dynamic data • source("SVMRank-Results-D.R"), to rank the interactions (again this needs to be done separately for different kinds of SA methods), • use source("Combine-Time-files.R"), if computing indices separately via previous file, • source("Sort-n-Plot-D.R") to sort the interactions. Note that the sorting is changes the interaction ranking in time. Thus • use source("Interaction-Priority-Intime.R") to find the prioritized ranking of each and every interaction over the different time points and finally • use source("Print-Ranking-AND-Interaction-Rank.R") to print individual ranking of the required input factor with other interaction factors.

## 6. Results & Discussion

### 6.1. Time series data by Gujral and MacBeath [1]

NOTE - Ranking was assigned on scores that were sorted in DECREASING values. So, 1 was assigned to highest score and vice versa.

Results for the 3<sup>rd</sup> order interactions are presented here. The results first discuss the behaviour of interactions across the snapshots of time using the computed sensitivities on fold change measurements per time snapshot. The analysis was done using 4 different sensitivity indices. Out of the  $^{71}C_3$  combinations, I consider/present only those combinations that show a ranking within first 10,000 out of 57,155. This choice is liberal and biologists/oncologists can have a more stricter choice as per need. Two observations are made, • the ranking of a particular combination is conserved (i.e within the 10,000 range) in a particular time point or in the early phase or late phase of WNT3A stimulation, across the majority of the four sensitivity methods, which is a strict criteria of assessment or • the ranking of a particular combination is conserved across time points/phase (i.e they are within the 10,000 range) and the majority of the four sensitivity methods, which is relaxed criteria of assessment. Applying this filter helps reveal important combinations of interest that might be working synergistically at a higher order level in the cell.

Regarding technical points of implementation, the rankings were generated without scaling/normalizing the time series data provided by Gujral and MacBeath [1]. For estimating the sensitivity indices, a small gaussian distribution using the function **rnorm** that generates a vector of normally distributed random variables given a vector length n (here 9, the 10th one is the mean/recorded gene regulation itself), a population mean  $\mu$  and population standard deviation  $\sigma$ . The syntax for using rnorm is as follows: **rnorm(n, mean, sd)**. Further, I use the **jitter** function to add a little bit of noise to the data. This helps to see if the generated rankings are robust or not.

### 6.2. Enumeration and ranking of 2415 PPP2R1A-X-X combinations from Gujral and MacBeath [1]

In the supplementary section, I present four files, each containing the rankings of 3rd order combinations, that vary in time (shown for 5 time points). Each file represents the rankings computed using a particular sensitivity method. The changing rankings in time for a particular combination represents the importance of contribution/role that combination plays in the cell stimulated with WNT3A. The sensitivity methods used are Hilbert Schmidt Independence Criterion indices (HSIC) indices (with rbf and linear kernel in Da Veiga [12]) and Sobol indices (with 2002 implementation in Saltelli [13] and martinez implementation in Martinez [14] and Baudin et al. [15]).

### 6.3. Conserved machine learning rankings for tested PPP2R1A-X-X combinations

A total of 2415, 3rd order combinations involving PPP2R1A were obtained from a full set of  $^{71}C_3 = 57155$  combinations. Further, from this selected set, using the above cri-

teria for conserved rankings, I report/tabulate the meaningful combinations that might be working synergistically. Tables 2, 3 and 4 show the rankings for the same combinations as in table 1, but using rbf kernel for HSIC, 2002 implementation for SOBOL and martinez implementation for SOBOL, respectively. As one tallies the rankings of across these tables for a particular combination, one finds that the role of the combination of interest is conserved. This conservation points to the existence of the biological synergy, whether the combination has been tested or unexplored/untested.

### 6.3.1. Examining the behaviour of PPP2CA-PPP2R1A-X combinations

Goudreault et al. [16] indicate that the PP2A catalytic (PP2A-C) subunit binds directly to the PP2A-A scaffolding subunit (two 85% identical proteins, PP2A-A $\alpha$  and PP2A-A $\beta$ , are present in human cells), to form the PP2A dimeric core. This core serves as a platform for the association of a regulatory or B subunit to generate a trimeric complex important for substrate recruitment and subcellular targeting.

The core enzyme of PP2A comprises a 65 kDa scaffolding subunit and a 36 kDa catalytic subunit. Xing et al. [17] report the crystal structures of the PP2A core enzyme bound to two of its inhibitors. They observe that the catalytic subunit recognizes one end of the elongated scaffolding subunit by interacting with the conserved ridges of HEAT repeats 11-15. Formation of the core enzyme forced the scaffolding subunit to undergo pronounced structural rearrangement. The scaffolding subunit exhibited considerable conformational flexibility, which is proposed to play an essential role in PP2A function. These structures, together with biochemical analyses, revealed significant insights into PP2A function and serve as a framework for deciphering the diverse roles of PP2A in cellular physiology. Further, inactivation of both the  $\alpha$  and  $\beta$  isoforms of the PP2A scaffolding subunit has been linked to cancer. They cite various references where mutations in the scaffolding subunit result in compromised binding to the regulatory or catalytic subunit of PP2A or a total absence or substantial reduction of the scaffolding subunit, which are closely associated with a variety of primary human tumors.

PPP2R1A is the predominant PP2A scaffold A-subunit that is required for functional PP2A complex formation. Kauko et al. [18] observed that unlike depletion of the catalytic PP2A subunit PPP2CA, siRNA of PPP2R1A did not cause cell lethality and, on the other hand, did not affect the PPP2CA expression. However, and as expected, PPP2R1A depletion resulted in destabilization of PPP2R5A (B56) and PPP2R2A (B55) B-subunits. Their results confirmed that PPP2R1A depletion results in comprehensive PP2A complex inhibition.

One finds the following combinations for PPP2CA along with PPP2R1A, to be prominent at 3rd order level - LEF1-PPP2CA-PPP2R1A, FZD7-PPP2CA-PPP2R1A, PPP2CA-PPP2R1A-FBXW4, NKD1-PPP2CA-PPP2R1A, PPP2CA-PPP2R1A-SEN2, PPP2CA-PPP2R1A-TLE2, PPP2CA-PPP2R1A-WNT5A, PPP2CA-PPP2R1A-WNT3A, KREMEN1-PPP2CA-PPP2R1A, FZD5-PPP2CA-PPP2R1A, DVL1-PPP2CA-PPP2R1A, GSK3A-PPP2CA-PPP2R1A, AES-PPP2CA-PPP2R1A, AXIN1-PPP2CA-PPP2R1A, EP300-PPP2CA-PPP2R1A, CCND2-PPP2CA-PPP2R1A, PPP2CA-PPP2R1A-WNT2B, FOXN1-PPP2CA-PPP2R1A, FZD1-PPP2CA-PPP2R1A, PPP2CA-PPP2R1A-TCF7, DAAM1-PPP2CA-PPP2R1A, CXXC4-PPP2CA-PPP2R1A, FBXW11-PPP2CA-PPP2R1A, APC-PPP2CA-PPP2R1A, DVL2-PPP2CA-PPP2R1A, FZD6-PPP2CA-PPP2R1A, FBXW2-

RANKING @ $t_i$ USING HSIC - LINEAR												
3rd order comb.	$t_1$	$t_3$	$t_6$	$t_{12}$	$t_{24}$	3rd order comb.	$t_1$	$t_3$	$t_6$	$t_{12}$	$t_{24}$	
CSNK1D-FGF4-PPP2R1A	72	17401	22364	53716	30729	FSHB-NKD1-PPP2R1A	134	11978	48147	4744	11658	
FOXN1-KREMEN1-PPP2R1A	187	38390	45372	22596	7296	FSHB-FZD2-PPP2R1A	216	20883	30530	35125	19903	
CTNNB1P1-JUN-PPP2R1A	222	17930	41664	52992	44848	CCND1-FGF4-PPP2R1A	231	42431	52577	39266	5985	
CXXC4-FOSL1-PPP2R1A	255	24314	35136	31526	39110	FOSL1-PPP2R1A-SEN2	256	39545	1842	16944	18375	
DKK1-JUN-PPP2R1A	267	12255	56230	48454	54215	FRZB-GSK3A-PPP2R1A	353	14275	17584	12248	25992	
CSNK2A1-CTBP1-PPP2R1A	386	22561	33967	27086	25647	DAAM1-FGF4-PPP2R1A	419	31801	52927	54325	31945	
CXXC4-PORCN-PPP2R1A	424	27798	37533	50501	37618	DKK1-PPP2R1A-SEN2	442	14095	52078	45675	54675	
AES-FOXN1-PPP2R1A	486	23646	9985	11397	37399	DVL2-JUN-PPP2R1A	555	45651	45029	17035	30388	
AES-AXIN1-PPP2R1A	562	47451	24435	49898	51110	LEF1-NKD1-PPP2R1A	793	3084	55944	23057	25903	
FZD8-PORCN-PPP2R1A	807	27524	31540	26322	40650	FOSL1-PPP2R1A-RHOU	846	41555	5035	55239	46031	
FBXW11-LRP6-PPP2R1A	920	16519	19037	17797	45281	CSNK1G1-FOXN1-PPP2R1A	960	4562	8931	10045	26824	
CTNNB1-FOXN1-PPP2R1A	966	1729	7371	11775	25639	CSNK1D-PPP2R1A-WNT5A	992	931	1207	30631	56811	
PTX2-PORCN-PPP2R1A	1003	8071	39783	44256	5481	FBXW11-FGF4-PPP2R1A	1030	29187	47593	48874	21413	
CXXC4-FGF4-PPP2R1A	1044	30931	36251	44472	52608	CSNK1D-PPP2R1A-TCF7L1	1128	12625	3602	38061	56712	
LEF1-PORCN-PPP2R1A	1139	34004	43790	26178	5620	CCND1-CTBP1-PPP2R1A	1192	36857	14658	39423	20532	
DKK1-FGF4-PPP2R1A	1228	16772	51023	37645	49558	FZD1-PORCN-PPP2R1A	1234	19388	36871	41947	10191	
DVL1-FOXN1-PPP2R1A	1316	40931	10069	3721	36477	PPP2R1A-WNT1-WNT4	1345	13482	18287	10132	56367	
DVL2-FGF4-PPP2R1A	1363	45199	42753	22929	46333	CSNK1D-PPP2R1A-TCF7	1430	4169	153	38743	7414	
CSNK2A1-MYC-PPP2R1A	1454	17389	25178	16938	14057	FBXW11-FOXN1-PPP2R1A	1485	2012	6552	10843	25217	
CTBP1-FGF4-PPP2R1A	1692	30523	34482	40227	19588	FBXW2-FGF4-PPP2R1A	1759	32973	44562	51245	8907	
CSNK2A1-FOXN1-PPP2R1A	1773	10252	16688	5889	9126	CXXC4-JUN-PPP2R1A	1782	11540	37923	13434	43762	
PPP2R1A-WNT3-WNT3A	1817	55448	5096	45267	43648	CSNK2A1-FGF4-PPP2R1A	1819	25704	42101	34434	17125	
FRZB-PORCN-PPP2R1A	1881	14863	41848	44601	12655	AXIN1-FOXN1-PPP2R1A	1913	4756	8847	11042	32343	
FOSL1-PPP2R1A-SFRP4	1952	52448	1955	16120	30096	CSNK1G1-JUN-PPP2R1A	1986	10228	52696	13904	47706	
LEF1-MYC-PPP2R1A	1990	40461	15570	31458	22391	FBXW11-JUN-PPP2R1A	2029	7720	56156	47859	37754	
FZD2-PORCN-PPP2R1A	2085	13234	40114	30182	21029	CCND3-PORCN-PPP2R1A	2099	25783	29032	23766	18843	
CSNK1A1-FGF4-PPP2R1A	2100	34624	20608	35480	22746	DKK1-GSK3A-PPP2R1A	2104	13726	28756	56201	53104	
DIXDC1-NKD1-PPP2R1A	2140	5484	54992	25998	568	FZD6-PORCN-PPP2R1A	2181	22169	35065	11807	6867	
FZD1-JUN-PPP2R1A	2184	21063	36959	28810	6175	BCL9-FGF4-PPP2R1A	2209	19748	39118	49100	20100	
FZD5-PPP2R1A-WNT5A	2239	9275	9172	22179	32268	FSHB-GSK3A-PPP2R1A	2267	11196	31968	18565	24240	
PPP2R1A-WNT3-WNT4	2411	43365	6520	45456	48427	FRAT1-JUN-PPP2R1A	2465	21726	41887	23096	41465	
FBXW11-FZD2-PPP2R1A	2469	12611	33445	15277	21128	DAAM1-GSK3A-PPP2R1A	2495	39121	35124	30013	51000	
CSNK1G1-FGF4-PPP2R1A	2535	19539	51865	57137	46652	PPP2R1A-TLE1-TLE2	2603	23452	51446	28086	54181	
FZD8-JUN-PPP2R1A	2633	37008	34949	19872	55616	APC-FZD6-PPP2R1A	2668	19187	290	54948	5882	
FOXN1-JUN-PPP2R1A	2696	46872	41797	35276	27908	CSNK1G1-PORCN-PPP2R1A	2697	18740	49826	20704	24737	
CCND2-LRP6-PPP2R1A	2763	48463	13066	23230	6578	DKK1-FOXN1-PPP2R1A	2783	23484	22053	10586	44403	
CSNK2A1-GSK3A-PPP2R1A	2846	28306	32715	6544	36708	CSNK1D-PORCN-PPP2R1A	2896	17111	34991	43683	19157	
PPP2R1A-TLE1-WNT4	2902	4217	52852	23987	31073	CTNNB1P1-FGF4-PPP2R1A	2959	22853	37005	28725	35681	
PPP2R1A-WNT1-WNT3A	2989	13277	15619	27990	53390	BCL9-PORCN-PPP2R1A	3009	23888	28332	49136	12024	
FGF4-PPP2R1A-SFRP4	3037	8718	1707	14759	34549	EP300-FOXN1-PPP2R1A	3054	31254	9485	1045	4738	
FZD1-NLK-PPP2R1A	3063	6647	16715	10003	26509	DAAM1-FOXN1-PPP2R1A	3097	26397	35409	10550	45683	
PPP2R1A-SFRP1-TCF7	3233	44109	34973	47932	35401	DVL1-FGF4-PPP2R1A	3242	41242	45411	17324	23922	
FZD7-PORCN-PPP2R1A	3293	54918	29516	41742	23131	FZD5-FGF4-PPP2R1A	3315	19006	41149	46199	17261	
FOSL1-PORCN-PPP2R1A	3418	54803	40086	41005	20335	FBXW11-GSK3A-PPP2R1A	3471	17513	23616	47087	26387	
AXIN1-FZD2-PPP2R1A	3530	36160	24224	14226	14076	DVL1-GSK3A-PPP2R1A	3570	44275	16001	23234	34855	
EP300-PORCN-PPP2R1A	3588	55435	38638	36180	44771	FBXW11-PORCN-PPP2R1A	3600	13551	28934	48860	10946	
PPP2R1A-SFRP1-FBXW4	3602	34385	50714	10310	44807	FZD5-NKD1-PPP2R1A	3621	21515	54524	36048	1557	
CTNNB1-PORCN-PPP2R1A	3628	8334	43683	23768	39432	FRAT1-PORCN-PPP2R1A	3641	17091	37502	41949	11356	
DAAM1-PORCN-PPP2R1A	3682	30772	17215	29018	29847	CCND1-JUN-PPP2R1A	3683	12869	49497	55359	13160	
LRP5-NLK-PPP2R1A	3749	6866	25722	95	55900	CSNK1G1-NLK-PPP2R1A	3754	21618	10600	22928	48421	
CCND3-PPP2R1A-SEN2	3947	20724	4140	11034	41552	DKK1-PORCN-PPP2R1A	4028	22121	57008	12032	54395	
EP300-FGF4-PPP2R1A	4059	54172	38740	54434	30530	GSK3B-LRP6-PPP2R1A	4082	43470	10296	43375	25140	
EP300-JUN-PPP2R1A	4089	45635	48485	28347	10942	FZD5-PORCN-PPP2R1A	4090	33288	41287	38390	34991	
FRAT1-NLK-PPP2R1A	4096	7150	14882	4380	42041	CTBP1-PPP2R1A-TCF7	4108	3719	931	22058	13655	
CSNK2A1-NKD1-PPP2R1A	4118	2001	56920	13318	8736	CTNNB1P1-NLK-PPP2R1A	4168	17696	21970	43414	47292	
DKK1-PPP2R1A-TLE2	4213	1676	48827	40467	57091	CTNNB1P1-FRAT1-PPP2R1A	4272	14548	33170	16600	48598	
CTBP1-GSK3A-PPP2R1A	4275	19056	10307	24065	37785	GSK3B-JUN-PPP2R1A	4299	50524	49319	35755	3146	
PPP2R1A-TLE1-WIF1	4307	33741	44977	32847	32390	DIXDC1-FOXN1-PPP2R1A	4318	4042	7718	10315	5136	
PPP2R1A-SFRP1-WNT3A	4336	49933	48304	18593	24856	FZD7-JUN-PPP2R1A	4369	47090	33547	30519	53889	
BCL9-JUN-PPP2R1A	4379	12860	38522	50713	4351	CSNK1A1-PORCN-PPP2R1A	4422	33823	41491	28773	10648	
CXXC4-PPP2R1A-RHOU	4427	19193	3464	42655	56387	FOSL1-PPP2R1A-TCF7	4468	34122	1739	41424	25089	
FZD8-GSK3A-PPP2R1A	4484	40441	18881	46804	54756	PPP2R1A-RHOU-SLC9A3R1	4485	42742	45200	38226	53842	
DKK1-PPP2R1A-WNT5A	4534	3478	36759	50853	55700	FZD1-NKD1-PPP2R1A	4562	26290	43026	35994	1774	

Table 1: Rankings of PPP2R1A-X-X. A list of approximately first 125 combinations with rankings below 10,000 out of 57,155. SA - HSIC; Kernel - linear

PPP2CA-PPP2R1A, CSNK2A1-PPP2CA-PPP2R1A, CTNNB1-PPP2CA-PPP2R1A, FOSL1-PPP2CA-PPP2R1A, LRP5-PPP2CA-PPP2R1A, FZD8-PPP2CA-PPP2R1A, MYC-PPP2CA-PPP2R1A, CSNK1D-PPP2CA-PPP2R1A, PPP2CA-PPP2R1A-PYGO1, PORCN-PPP2CA-PPP2R1A, FRAT1-PPP2CA-PPP2R1A, JUN-PPP2CA-PPP2R1A, CTBP1-PPP2CA-



RANKING @ $t_f$ USING HSIC - RBF											
3rd order comb.	$t_1$	$t_3$	$t_6$	$t_{12}$	$t_{24}$	3rd order comb.	$t_1$	$t_3$	$t_6$	$t_{12}$	$t_{24}$
CSNK1D-FGF4-PPP2R1A	3004	29048	12442	15684	23801	FSHB-NKD1-PPP2R1A	25236	3206	25555	29398	54336
FOXN1-KREMEN1-PPP2R1A	21547	15130	581	7154	55001	FSHB-FZD2-PPP2R1A	10535	30086	26859	11239	24594
CTNNBIP1-JUN-PPP2R1A	42662	30325	24952	5762	37211	CCND1-FGF4-PPP2R1A	9841	27457	12592	18053	2791
CXXC4-FOSL1-PPP2R1A	52227	34156	6226	46113	43359	FOSL1-PPP2R1A-SENP2	36531	47500	56688	1297	8711
DKK1-JUN-PPP2R1A	19726	15606	1085	29841	36603	FRZB-GSK3A-PPP2R1A	1658	24598	48047	40183	47791
CSNK2A1-CTBP1-PPP2R1A	51425	30212	13474	42814	33263	DAAM1-FGF4-PPP2R1A	1363	39705	27194	16188	12922
CXXC4-PORCN-PPP2R1A	20998	30567	5511	22186	56640	DKK1-PPP2R1A-SENP2	4320	17195	24869	14464	3866
AES-FOXN1-PPP2R1A	723	21691	22365	18788	29319	DVL2-JUN-PPP2R1A	7790	48428	6855	9490	40633
AES-AXIN1-PPP2R1A	37649	36390	27090	29535	33374	LEF1-NKD1-PPP2R1A	24944	9286	39491	44583	37109
FZD8-PORCN-PPP2R1A	3136	21194	9602	10973	55135	FOSL1-PPP2R1A-RHOU	19254	49825	54278	50968	41085
FBXW11-LRP6-PPP2R1A	2990	7171	41891	45594	39934	CSNK1G1-FOXN1-PPP2R1A	3415	1125	22606	474	39586
CTNNB1-FOXN1-PPP2R1A	6266	597	36708	568	27942	CSNK1D-PPP2R1A-WNT5A	27528	4279	14277	4265	42405
PITX2-PORCN-PPP2R1A	11355	50277	26063	28070	55628	FBXW11-FGF4-PPP2R1A	2311	3713	32222	41780	18993
CXXC4-FGF4-PPP2R1A	1192	9614	5570	26405	23051	CSNK1D-PPP2R1A-TCF7L1	34388	5648	48876	25681	52823
LEF1-PORCN-PPP2R1A	9650	37275	29706	14200	48587	CCND1-CTBP1-PPP2R1A	42960	11026	30626	24182	7494
DKK1-FGF4-PPP2R1A	1885	5747	727	4631	30783	FZD1-PORCN-PPP2R1A	24806	24942	1636	2232	55350
DVL1-FOXN1-PPP2R1A	7337	28739	5315	11310	23091	PPP2R1A-WNT1-WNT4	13056	3776	48355	444	25289
DVL2-FGF4-PPP2R1A	3678	46957	3278	19048	26196	CSNK1D-PPP2R1A-TCF7	34317	14103	3740	45791	33515
CSNK2A1-MYC-PPP2R1A	8973	18254	44398	29894	43896	FBXW11-FOXN1-PPP2R1A	848	15861	49514	22629	20720
CTBP1-FGF4-PPP2R1A	2812	38280	137	44051	39921	FBXW2-FGF4-PPP2R1A	849	18830	22979	9327	14927
CSNK2A1-FOXN1-PPP2R1A	647	14324	25472	4074	30161	CXXC4-JUN-PPP2R1A	8147	19410	4343	32567	48732
PPP2R1A-WNT3-WNT3A	9441	54192	34392	53766	7535	CSNK2A1-FGF4-PPP2R1A	166	29600	18823	44833	19787
FRZB-PORCN-PPP2R1A	13914	23845	13959	7815	56301	AXIN1-FOXN1-PPP2R1A	12949	15322	34068	9033	35734
FOSL1-PPP2R1A-SFRP4	50064	57024	56666	31648	53883	CSNK1G1-JUN-PPP2R1A	2410	8342	5954	20586	31871
LEF1-MYC-PPP2R1A	5271	38043	45068	15629	15850	FBXW11-JUN-PPP2R1A	15642	5206	44646	46199	19057
FZD2-PORCN-PPP2R1A	335	12575	8770	1810	55522	CCND3-PORCN-PPP2R1A	23176	16220	12632	6835	44417
CSNK1A1-FGF4-PPP2R1A	4863	12539	3164	12998	34074	DKK1-GSK3A-PPP2R1A	37	15243	34284	9621	35620
DIXDC1-NKD1-PPP2R1A	41282	2633	37452	52221	22216	FZD6-PORCN-PPP2R1A	23	17577	25321	670	56053
FZD1-JUN-PPP2R1A	32015	23065	8067	12950	35467	BCL9-FGF4-PPP2R1A	10398	5395	4459	43209	26087
FZD5-PPP2R1A-WNT5A	17060	9682	37942	54060	54700	FSHB-GSK3A-PPP2R1A	2994	22740	47062	16574	48029
PPP2R1A-WNT3-WNT4	6466	47384	44643	26384	8285	FRAT1-JUN-PPP2R1A	14775	16627	12246	41797	26468
FBXW11-FZD2-PPP2R1A	8700	4798	40674	36207	15746	DAAM1-GSK3A-PPP2R1A	6522	35629	52023	19728	17125
CSNK1G1-FGF4-PPP2R1A	8938	29139	2598	16353	38899	PPP2R1A-TLE1-TLE2	44598	3120	16931	19408	1179
FZD8-JUN-PPP2R1A	7769	37927	11864	24690	38173	APC-FZD6-PPP2R1A	26156	38611	29925	13305	29320
FOSL1-JUN-PPP2R1A	20816	55928	16147	47523	47242	CSNK1G1-PORCN-PPP2R1A	16024	19421	9392	5370	55173
CCND2-LRP6-PPP2R1A	7525	49696	47315	30017	29589	DKK1-FOXN1-PPP2R1A	1768	15517	15329	5073	18412
CSNK2A1-GSK3A-PPP2R1A	6662	21693	51937	52594	38018	CSNK1D-PORCN-PPP2R1A	16940	28022	22571	2476	54099
PPP2R1A-TLE1-WNT4	34919	1417	25861	8678	8293	CTNNBIP1-FGF4-PPP2R1A	2426	9206	12675	669	32498
PPP2R1A-WNT1-WNT3A	2644	9345	37570	29489	17577	BCL9-PORCN-PPP2R1A	28259	20478	5854	26873	52990
FGF4-PPP2R1A-SFRP4	8036	9755	54750	29227	49177	EP300-FOXN1-PPP2R1A	1354	35385	45759	2306	27930
FZD1-NLK-PPP2R1A	20834	8886	52092	12766	24248	DAAM1-FOXN1-PPP2R1A	1334	13230	49009	5916	8662
PPP2R1A-SFRP1-TCF7	8562	33991	8051	54700	29578	DVL1-FGF4-PPP2R1A	5991	18327	77	43200	54479
FZD7-PORCN-PPP2R1A	39388	55931	21995	3462	52550	FZD5-FGF4-PPP2R1A	1273	30877	9798	36227	30025
FOSL1-PORCN-PPP2R1A	1690	56373	15424	4340	55845	FBXW11-GSK3A-PPP2R1A	2166	8382	55946	44477	32821
AXIN1-FZD2-PPP2R1A	26985	37883	10434	10353	20291	DVL1-GSK3A-PPP2R1A	15051	28660	39098	46332	48932
EP300-PORCN-PPP2R1A	9705	56176	25373	738	50930	FBXW11-PORCN-PPP2R1A	5633	5510	29166	19086	52513
PPP2R1A-SFRP1-FBXW4	43447	35660	2162	20015	15609	FZD5-NKD1-PPP2R1A	23335	9105	47323	31744	56453
CTNNB1-PORCN-PPP2R1A	12296	20951	22147	236	56429	FRAT1-PORCN-PPP2R1A	14510	12147	3493	8420	55974
DAAM1-PORCN-PPP2R1A	43717	12829	27614	274	42068	CCND1-JUN-PPP2R1A	28970	7761	24201	8661	5096
LRP5-NLK-PPP2R1A	22739	10079	12169	17484	38120	CSNK1G1-NLK-PPP2R1A	35195	9424	21823	20710	43474
CCND3-PPP2R1A-SENP2	10144	14970	33230	89	13210	DKK1-PORCN-PPP2R1A	15567	20860	1442	5709	55732
EP300-FGF4-PPP2R1A	434	56284	13608	15792	27194	GSK3B-LRP6-PPP2R1A	6362	47681	43483	14542	49585
EP300-JUN-PPP2R1A	5997	52619	15125	40032	31600	FZD5-PORCN-PPP2R1A	23669	41306	11440	2543	56519
FRAT1-NLK-PPP2R1A	47257	5675	39028	27369	25057	CTBP1-PPP2R1A-TCF7	13922	7113	7010	44002	53010
CSNK2A1-NKD1-PPP2R1A	19188	9240	34119	49629	44582	CTNNBIP1-NLK-PPP2R1A	27842	23336	43647	19091	40032
DKK1-PPP2R1A-TLE2	18876	4979	33058	36302	34591	CTNNBIP1-FRAT1-PPP2R1A	19452	31715	19287	3657	50902
CTBP1-GSK3A-PPP2R1A	193	46150	47414	42441	47384	GSK3B-JUN-PPP2R1A	4762	52417	19413	19919	45463
PPP2R1A-TLE1-WIF1	18734	28938	477	39566	970	DIXDC1-FOXN1-PPP2R1A	3585	17552	18249	8440	13079
PPP2R1A-SFRP1-WNT3A	10638	51919	14638	49471	17076	FZD7-JUN-PPP2R1A	15754	47453	8319	37051	11201
BCL9-JUN-PPP2R1A	38825	31345	7280	45954	33797	CSNK1A1-PORCN-PPP2R1A	32307	17216	8460	87	56661
CXXC4-PPP2R1A-RHOU	24725	6975	48923	38600	48066	FOSL1-PPP2R1A-TCF7	32156	40396	19240	52936	29464
FZD8-GSK3A-PPP2R1A	442	39080	49490	18545	37574	PPP2R1A-RHOU-SLC9A3R1	50539	48128	21287	4442	19281
DKK1-PPP2R1A-WNT5A	17268	5548	34963	48461	43857	FZD1-NKD1-PPP2R1A	38340	8464	17462	30009	50089

Table 2: Rankings of PPP2R1A-X-X. A list of approximately first 125 combinations with rankings below 10,000 out of 57,155. SA - HSIC; Kernel - rbf

PPP2R1A, CTNNBIP1-PPP2CA-PPP2R1A, FGF4-PPP2CA-PPP2R1A, CSNK1A1-PPP2CA-PPP2R1A, CCND1-PPP2CA-PPP2R1A, PPP2CA-PPP2R1A-T, and NLK-PPP2CA-PPP2R1A. All these combinations indicate the existence of a possible synergy when they take a higher rank in the list of combinations (Table not shown, but data available in supplementary files).

RANKING @ $t_1$ USING SOBOLE - 2002												
3rd order comb.	$t_1$	$t_3$	$t_6$	$t_{12}$	$t_{24}$	3rd order comb.	$t_1$	$t_3$	$t_6$	$t_{12}$	$t_{24}$	
CSNK1D-FGF4-PPP2R1A	16041	36350	23034	23038	36186	FSHB-NKD1-PPP2R1A	46297	55865	50849	48169	20237	
FOXN1-KREMEN1-PPP2R1A	42868	43393	35692	37283	25597	FSHB-FZD2-PPP2R1A	42041	22925	48680	43398	7266	
CTNNB1P1-JUN-PPP2R1A	55954	42703	38291	39039	13787	CCND1-FGF4-PPP2R1A	8041	6110	9333	3122	15526	
CXXC4-FOSL1-PPP2R1A	33024	20784	45045	33319	8066	FOSL1-PPP2R1A-SENP2	17310	2495	82	9104	48865	
DKK1-JUN-PPP2R1A	57057	38094	40889	35645	26618	FRZB-GSK3A-PPP2R1A	25879	15158	11743	5128	42437	
CSNK2A1-CTBP1-PPP2R1A	9565	3272	9580	22975	53995	DAAM1-FGF4-PPP2R1A	15916	6776	25382	1808	40386	
CXXC4-PORCN-PPP2R1A	44156	3317	53822	38916	15985	DKK1-PPP2R1A-SENP2	32867	41750	37757	38732	22794	
AES-FOXN1-PPP2R1A	41646	39241	36628	36288	5132	DVL2-JUN-PPP2R1A	32860	32858	41918	49574	8979	
AES-AXIN1-PPP2R1A	17980	11690	1667	25620	39308	LEF1-NKD1-PPP2R1A	9769	22805	4489	9080	56436	
FZD8-PORCN-PPP2R1A	38026	11841	38929	49830	12841	FOSL1-PPP2R1A-RHOU	40904	5712	55181	51304	16176	
FBXW11-LRP6-PPP2R1A	33578	51917	41394	41899	136	CSNK1G1-FOXN1-PPP2R1A	26102	33906	21109	71	51037	
CTNNB1-FOXN1-PPP2R1A	25582	48808	11814	14904	35610	CSNK1D-PPP2R1A-WNT5A	26135	44357	28294	20860	36948	
PITX2-PORCN-PPP2R1A	10644	13926	20214	8562	45301	FBXW11-FGF4-PPP2R1A	21525	6774	7962	683	32733	
CXXC4-FGF4-PPP2R1A	6382	430	21801	13251	51268	CSNK1D-PPP2R1A-TCF7L1	25967	41054	27430	10798	32868	
LEF1-PORCN-PPP2R1A	55205	5382	39482	30816	5128	CCND1-CTBP1-PPP2R1A	6841	4832	18010	2548	48027	
DKK1-FGF4-PPP2R1A	324	9809	21588	1227	46038	FZD1-PORCN-PPP2R1A	30101	12907	33213	40879	17697	
DVL1-FOXN1-PPP2R1A	51816	4887	37165	29807	19052	PPP2R1A-WNT1-WNT4	11965	38223	20939	13880	37473	
DVL2-FGF4-PPP2R1A	28562	7712	15949	10339	52618	CSNK1D-PPP2R1A-TCF7	41472	28978	28805	36435	24561	
CSNK2A1-MYC-PPP2R1A	43792	409	55826	32832	9529	FBXW11-FOXN1-PPP2R1A	37757	51830	45317	45654	30175	
CTBP1-FGF4-PPP2R1A	6809	2544	11557	11279	21648	FBXW2-FGF4-PPP2R1A	24138	8011	10235	12268	48408	
CSNK2A1-FOXN1-PPP2R1A	48112	40897	44318	33462	5020	CXXC4-JUN-PPP2R1A	44274	1712	51774	45829	14514	
PPP2R1A-WNT3-WNT3A	36443	18940	41310	53135	2959	CSNK2A1-FGF4-PPP2R1A	14590	280	8154	14376	57124	
FRZB-PORCN-PPP2R1A	30075	7164	33481	29288	19966	AXIN1-FOXN1-PPP2R1A	44944	9431	31934	45514	23258	
FOSL1-PPP2R1A-SFRP4	11157	1063	12252	1915	27364	CSNK1G1-JUN-PPP2R1A	17390	9694	2316	9148	46335	
LEF1-MYC-PPP2R1A	49356	45923	37942	29145	1127	FBXW11-JUN-PPP2R1A	30442	37428	31872	51853	5287	
FZD2-PORCN-PPP2R1A	30442	37428	31872	51853	5287	CCND3-PORCN-PPP2R1A	36499	25184	35693	45688	32879	
CSNK1A1-FGF4-PPP2R1A	19430	15108	26384	3273	35844	DKK1-GSK3A-PPP2R1A	3576	54378	12570	4237	42868	
DIXDC1-NKD1-PPP2R1A	43958	23448	33394	28989	46225	FZD6-PORCN-PPP2R1A	57022	5258	35690	36036	2340	
FZD1-JUN-PPP2R1A	41482	46290	33964	52529	4744	BCL9-FGF4-PPP2R1A	44107	9923	39133	46912	21549	
FZD5-PPP2R1A-WNT5A	13161	3675	15841	13079	29407	FSHB-GSK3A-PPP2R1A	49293	47302	38519	53839	5159	
PPP2R1A-WNT3-WNT4	16616	40261	2791	2571	54999	FRAT1-JUN-PPP2R1A	42706	1201	38950	37080	1437	
FBXW11-FZD2-PPP2R1A	18515	35966	25544	19946	46068	DAAM1-GSK3A-PPP2R1A	10125	15478	15201	12370	39692	
CSNK1G1-FGF4-PPP2R1A	48874	4935	46376	33919	6326	PPP2R1A-TLE1-TLE2	12057	33276	3659	23431	32864	
FZD8-JUN-PPP2R1A	37523	49992	44475	49521	6287	APC-FZD6-PPP2R1A	23330	27149	8978	18879	50391	
FOSL1-JUN-PPP2R1A	21985	646	17395	14514	28922	CSNK1G1-PORCN-PPP2R1A	15949	51267	916	23706	44599	
CCND2-LRP6-PPP2R1A	6444	7887	523	4254	56131	DKK1-FOXN1-PPP2R1A	53275	9764	33988	42162	49627	
CSNK2A1-GSK3A-PPP2R1A	11380	31286	12842	24412	45687	CSNK1D-PORCN-PPP2R1A	38585	10367	29409	42259	26713	
PPP2R1A-TLE1-WNT4	50847	17197	51184	35836	4656	CTNNB1P1-FGF4-PPP2R1A	21220	11125	5808	8971	47491	
PPP2R1A-WNT1-WNT3A	44486	25983	55160	38768	876	BCL9-PORCN-PPP2R1A	3726	55756	5699	8967	45381	
FGF4-PPP2R1A-SFRP4	41615	32421	55637	50004	3755	EP300-FOXN1-PPP2R1A	27453	4062	5453	17377	46862	
FZD1-NLK-PPP2R1A	24761	3213	17679	9061	47517	DAAM1-FOXN1-PPP2R1A	36154	7660	34600	37941	2552	
PPP2R1A-SFRP1-TCF7	38554	10598	51386	54486	17369	DVL1-FGF4-PPP2R1A	4058	49292	3312	1776	45495	
FZD7-PORCN-PPP2R1A	3455	13963	24568	11652	46242	FZD5-FGF4-PPP2R1A	8710	44431	13859	25041	47104	
FOSL1-PORCN-PPP2R1A	12329	10794	4983	7297	24630	FBXW11-GSK3A-PPP2R1A	23281	8449	7832	5700	53451	
AXIN1-FZD2-PPP2R1A	3497	36120	1619	4955	9233	DVL1-GSK3A-PPP2R1A	5159	17419	20417	26623	33226	
EP300-PORCN-PPP2R1A	22470	6955	21990	5623	28699	FBXW11-PORCN-PPP2R1A	30044	41098	40844	44354	36462	
PPP2R1A-SFRP1-FBXW4	14313	28307	8709	5545	45438	FZD5-NKD1-PPP2R1A	8457	17431	20808	3578	44409	
CTNNB1-FOXN1-PPP2R1A	22429	23850	2877	10330	35039	FRAT1-PORCN-PPP2R1A	40959	10690	33431	37055	7595	
DAAM1-PORCN-PPP2R1A	37641	4953	51858	42273	23084	CCND1-JUN-PPP2R1A	34114	4338	47559	54747	6240	
LRP5-NLK-PPP2R1A	3984	29481	13824	21011	33733	CSNK1G1-NLK-PPP2R1A	44178	38444	50560	39549	2806	
CCND3-PPP2R1A-SENP2	38063	23006	32403	43199	16700	DKK1-PORCN-PPP2R1A	49848	9076	45012	37637	2592	
EP300-FGF4-PPP2R1A	28963	23170	45747	34094	8154	GSK3B-LRP6-PPP2R1A	46339	44896	33944	47999	1990	
EP300-JUN-PPP2R1A	7366	1840	9839	10599	24170	FZD5-PORCN-PPP2R1A	40787	51757	29744	54782	6188	
FRAT1-NLK-PPP2R1A	28123	53372	22683	12683	35312	CTBP1-PPP2R1A-TCF7	49874	42210	43146	41646	23377	
CSNK2A1-NKD1-PPP2R1A	22699	6006	1296	8582	18490	CTNNB1P1-NLK-PPP2R1A	9258	4462	1417	3718	45909	
DKK1-PPP2R1A-TLE2	8680	19585	22562	17102	31812	CTNNB1P1-FRAT1-PPP2R1A	2661	17596	13691	9074	52194	
CTBP1-GSK3A-PPP2R1A	26233	34978	12162	4952	29857	GSK3B-JUN-PPP2R1A	47780	49037	35224	55410	30	
PPP2R1A-TLE1-WIF1	45090	23493	53498	33748	24410	DIXDC1-FOXN1-PPP2R1A	6911	39828	26802	5793	42038	
PPP2R1A-SFRP1-WNT3A	17421	39053	2157	2455	38476	FZD7-JUN-PPP2R1A	705	20290	26650	23750	28134	
BCL9-JUN-PPP2R1A	5492	16065	23828	22460	28747	CSNK1A1-PORCN-PPP2R1A	33540	14808	31151	43414	22297	
CXXC4-PPP2R1A-RHOU	242	49782	8767	11033	47691	FOSL1-PPP2R1A-TCF7	25440	6855	18711	224	45135	
FZD8-GSK3A-PPP2R1A	10013	21215	18756	2860	56157	PPP2R1A-RHOU-SLC9A3R1	18369	33943	3519	827	50991	
DKK1-PPP2R1A-WNT5A	4917	40830	24393	22265	31089	FZD1-NKD1-PPP2R1A	5966	22666	26851	20696	40193	

Table 3: Rankings of PPP2R1A-X-X. A list of approximately first 125 combinations with rankings below 10,000 out of 57,155. SA - SOBOLE; Implementation - 2002

## 6.4. Known PPP2CA-X combinations

Now, based on the formation of complex between PPP2CA and PPP2R1A, we also know that PPP2CA interacts with certain other genes/proteins. In a parallel manuscript in [https://osf.io/preprints/osf/ux57e\\_v1](https://osf.io/preprints/osf/ux57e_v1), possible 3rd order combinations

RANKING @ $t_i$ USING SOBOL - MARTINEZ												
3rd order comb.	$t_1$	$t_3$	$t_6$	$t_{12}$	$t_{24}$	3rd order comb.	$t_1$	$t_3$	$t_6$	$t_{12}$	$t_{24}$	
CSNK1D-FGF4-PPP2R1A	32236	18431	4861	24170	28783	FSHB-NKD1-PPP2R1A	53109	51767	230	25045	9445	
FOXN1-KREMEN1-PPP2R1A	9818	15093	45644	39058	38490	FSHB-FZD2-PPP2R1A	46195	47198	3580	18156	8533	
CTNNB1P1-JUN-PPP2R1A	53037	53341	798	1131	42840	CCND1-FGF4-PPP2R1A	12160	21244	47621	988	46218	
CXXC4-FOSL1-PPP2R1A	12098	31961	43639	23246	42209	FOSL1-PPP2R1A-SEN2P	53756	53724	17611	16937	2010	
DKK1-JUN-PPP2R1A	44652	4023	140	29083	28080	FRZB-GSK3A-PPP2R1A	3874	54884	15294	31066	53198	
CSNK2A1-CTBP1-PPP2R1A	8485	5851	54850	57106	50316	DAAM1-FGF4-PPP2R1A	8627	16017	17059	33072	42909	
CXXC4-PORCN-PPP2R1A	56184	21259	15139	35428	46765	DKK1-PPP2R1A-SEN2P	5672	4114	48876	17608	30388	
AES-FOXN1-PPP2R1A	41046	36730	9801	33717	13773	DVL2-JUN-PPP2R1A	47799	3904	40852	41830	40087	
AES-AXIN1-PPP2R1A	29709	7204	7179	22853	46549	LEF1-NKD1-PPP2R1A	2716	16678	11945	8557	27909	
FZD8-PORCN-PPP2R1A	8407	43072	773	21094	20949	FOSL1-PPP2R1A-RHOU	7680	16304	49608	19854	56661	
FBXW11-LRP6-PPP2R1A	46450	17620	23679	21851	45002	CSNK1G1-FOXN1-PPP2R1A	2180	53719	33104	7285	38261	
CTNNB1-FOXN1-PPP2R1A	42625	3532	15726	6439	5650	CSNK1D-PPP2R1A-WNT5A	34799	46397	27927	38367	6548	
PITX2-PORCN-PPP2R1A	28551	48685	56979	48784	335	FBXW11-FGF4-PPP2R1A	29450	15887	30155	5281	2799	
CXXC4-FGF4-PPP2R1A	8907	21944	29567	29533	9336	CSNK1D-PPP2R1A-TCF7L1	1420	17934	41275	37855	4684	
LEF1-PORCN-PPP2R1A	26478	55431	54500	47281	17795	CCND1-CTBP1-PPP2R1A	36220	16302	43805	43688	31549	
DKK1-FGF4-PPP2R1A	3005	47943	56596	50923	40368	FZD1-PORCN-PPP2R1A	14339	46256	12856	9505	14272	
DVL1-FOXN1-PPP2R1A	37862	23663	31790	1787	56934	PPP2R1A-WNT1-WNT4	37092	5843	25053	14666	48915	
DVL2-FGF4-PPP2R1A	4007	50952	55134	49671	15769	CSNK1D-PPP2R1A-TCF7	50128	22951	5812	8544	53759	
CSNK2A1-MYC-PPP2R1A	25664	26823	22802	51070	20795	FBXW11-FOXN1-PPP2R1A	48234	30804	26631	857	24851	
CTBP1-FGF4-PPP2R1A	29282	16738	9342	10907	44150	FBXW2-FGF4-PPP2R1A	33575	43903	12774	14307	1344	
CSNK2A1-FOXN1-PPP2R1A	45269	55820	45196	49391	8270	CXXC4-JUN-PPP2R1A	51605	35237	2	12177	38141	
PPP2R1A-WNT3-WNT3A	23525	2536	27665	46568	52987	CSNK2A1-FGF4-PPP2R1A	2708	11996	14685	9650	3147	
FRZB-PORCN-PPP2R1A	14737	40959	24690	53668	10525	AXIN1-FOXN1-PPP2R1A	8831	10151	38688	42230	32668	
FOSL1-PPP2R1A-SFRP4	40500	53353	26998	9354	15844	CSNK1G1-JUN-PPP2R1A	23606	19004	7535	6758	46881	
LEF1-MYC-PPP2R1A	11765	47450	24677	17153	11080	FBXW11-JUN-PPP2R1A	40438	49975	123	2090	49430	
FZD2-PORCN-PPP2R1A	36388	5831	12064	46816	7716	CCND3-PORCN-PPP2R1A	34741	27548	1460	1440	48656	
CSNK1A1-FGF4-PPP2R1A	23603	17704	17458	38201	8185	DKK1-GSK3A-PPP2R1A	54509	9044	42211	28127	48761	
DIXDC1-NKD1-PPP2R1A	12774	34350	23086	9498	28407	FZD6-PORCN-PPP2R1A	53027	30452	2523	3375	40591	
FZD1-JUN-PPP2R1A	55470	32960	48579	16406	13433	BCL9-FGF4-PPP2R1A	15072	47099	40017	23574	24903	
FZD5-PPP2R1A-WNT5A	24265	52942	6115	49206	3338	FSHB-GSK3A-PPP2R1A	37883	32032	13437	29910	10314	
PPP2R1A-WNT3-WNT4	38925	6831	8673	22959	7896	FRAT1-JUN-PPP2R1A	50324	54822	2963	10268	16810	
FBXW11-FZD2-PPP2R1A	14157	48722	2068	51470	35024	DAAM1-GSK3A-PPP2R1A	6061	17058	22794	19251	31262	
CSNK1G1-FGF4-PPP2R1A	51350	42511	16585	6456	20879	PPP2R1A-TLE1-TLE2	34102	7385	53917	17882	1521	
FZD8-JUN-PPP2R1A	13212	37713	26615	7532	10626	APC-FZD6-PPP2R1A	47750	6639	25002	27569	43398	
FOSL1-JUN-PPP2R1A	3192	33424	53266	44332	7085	CSNK1G1-PORCN-PPP2R1A	503	35730	3044	6124	43150	
CCND2-LRP6-PPP2R1A	22644	3731	31401	50028	44047	DKK1-FOXN1-PPP2R1A	11050	23384	35332	36428	15008	
CSNK2A1-GSK3A-PPP2R1A	1426	6407	17691	10783	1599	CSNK1D-PORCN-PPP2R1A	46494	24460	5959	26920	56966	
PPP2R1A-TLE1-WNT4	51244	380	10001	46733	50906	CTNNB1P1-FGF4-PPP2R1A	2386	11757	56920	53488	54014	
PPP2R1A-WNT1-WNT3A	43905	2516	24424	44521	46746	BCL9-PORCN-PPP2R1A	33142	27149	6583	54862	6499	
FGF4-PPP2R1A-SFRP4	7544	187	45686	38307	50947	EP300-FOXN1-PPP2R1A	2782	54679	56277	56440	4527	
FZD1-NLK-PPP2R1A	14161	20148	41005	22371	49081	DAAM1-FOXN1-PPP2R1A	16648	38866	37440	28676	56981	
PPP2R1A-SFRP1-TCF7	53553	348	40624	30419	18672	DVL1-FGF4-PPP2R1A	49459	28509	9009	47709	26114	
FZD7-PORCN-PPP2R1A	3429	55100	21500	6297	49234	FZD5-FGF4-PPP2R1A	12413	53064	13958	7044	29926	
FOSL1-PORCN-PPP2R1A	39998	53979	32389	7667	4764	FBXW11-GSK3A-PPP2R1A	9881	41814	51632	48357	45220	
AXIN1-FZD2-PPP2R1A	3953	44226	7710	12132	33158	DVL1-GSK3A-PPP2R1A	44873	9132	16734	30736	28754	
EP300-PORCN-PPP2R1A	27723	53765	27214	12840	4389	FBXW11-PORCN-PPP2R1A	31994	28809	36029	1772	30055	
PPP2R1A-SFRP1-FBXW4	49726	22554	15762	22294	1177	FZD5-NKD1-PPP2R1A	47879	55985	27626	45478	27533	
CTNNB1-PORCN-PPP2R1A	48141	50110	38901	17504	28601	FRAT1-PORCN-PPP2R1A	54020	46007	6706	6670	15729	
DAAM1-PORCN-PPP2R1A	23922	38071	32267	16742	32775	CCND1-JUN-PPP2R1A	30535	50399	37639	34913	21248	
LRP5-NLK-PPP2R1A	12943	44041	12550	26240	4030	CSNK1G1-NLK-PPP2R1A	20710	56117	30444	20124	29195	
CCND3-PPP2R1A-SEN2P	37199	29603	7973	16912	56468	DKK1-PORCN-PPP2R1A	20241	3736	5919	32750	36919	
EP300-FGF4-PPP2R1A	27200	21724	3067	2038	49507	GSK3B-LRP6-PPP2R1A	15655	30336	22632	52608	51848	
EP300-JUN-PPP2R1A	31760	54584	34286	9593	22982	FZD5-PORCN-PPP2R1A	52911	48660	11049	3529	40475	
FRAT1-NLK-PPP2R1A	81	37116	49362	15818	45457	CTBP1-PPP2R1A-TCF7	34072	35688	39822	101	34942	
CSNK2A1-NKD1-PPP2R1A	32525	9590	31893	25709	13680	CTNNB1P1-NLK-PPP2R1A	14880	54925	8361	17662	47801	
DKK1-PPP2R1A-TLE2	9107	54957	44853	50873	12590	CTNNB1P1-FRAT1-PPP2R1A	22487	8177	46965	50040	53950	
CTBP1-GSK3A-PPP2R1A	53371	32489	5597	28864	51119	GSK3B-JUN-PPP2R1A	18729	28467	34179	51065	34090	
PPP2R1A-TLE1-WIF1	41681	6027	12229	35646	49978	DIXDC1-FOXN1-PPP2R1A	17025	25373	2795	32623	47876	
PPP2R1A-SFRP1-WNT3A	42274	41607	49464	5882	1244	FZD7-JUN-PPP2R1A	51015	23106	55136	52607	4997	
BCL9-JUN-PPP2R1A	47302	45845	30052	50411	23968	CSNK1A1-PORCN-PPP2R1A	51187	35349	570	23329	56565	
CXXC4-PPP2R1A-RHOU	46930	17735	33762	56517	50128	FOSL1-PPP2R1A-TCF7	2723	11290	22180	19980	37136	
FZD8-GSK3A-PPP2R1A	43647	4293	7400	39908	40682	PPP2R1A-RHOU-SLC9A3R1	29657	56281	21280	4109	44433	
DKK1-PPP2R1A-WNT5A	50575	2419	39679	15768	20655	FZD1-NKD1-PPP2R1A	7873	44792	19632	50737	12728	

Table 4: Rankings of PPP2R1A-X-X. A list of approximately first 125 combinations with rankings below 10,000 out of 57,155. SA - SOBOL; Implementation - martinez

of PPP2CA have been documented, with citation of literature that refers to existing 2nd order combinations of PPP2CA. I use these documented 2nd order combinations of PPP2CA, and infer the possible combinations of PPP2R1A (tallied with genes/proteins that might form complex with PPP2CA-PPP2R1A, as mentioned in section 6.3.1 above), that might be working synergistically. The below sections, contain

combinations of PPP2R1A, that have a gene/protein that also associates with PPP2CA (see [https://osf.io/preprints/osf/ux57e\\_v1](https://osf.io/preprints/osf/ux57e_v1)).

#### **6.4.1. Examining the behaviour of AXIN-PPP2R1A-X combinations**

CONNECTION OF AXIN-PPP2CA - Willert et al. [19] show that AXIN is dephosphorylated in response to WNT signaling and the dephosphorylated AXIN binds  $\beta$ -catenin less efficiently than the phosphorylated form. Thus, WNT signaling lowered AXIN's affinity for  $\beta$ -catenin, thereby disengaging  $\beta$ -catenin from the degradation machinery. Ikeda et al. [20] show that the heterodimeric form of PP2A directly binds to AXIN, and PP2A complexed with AXIN dephosphorylated APC phosphorylated by GSK3 $\beta$ . Taken together, their results suggest that GSK3 $\beta$ -dependent phosphorylation of APC can be modulated by  $\beta$ -catenin and PP2A complexed with AXIN.

Looking at the tables above, one finds the following combinations for AXIN along with PPP2R1A, to be prominent at 3rd order level - AES-AXIN1-PPP2R1A, AXIN1-FZD2-PPP2R1A and AXIN1-FOXN1-PPP2R1A. All these combinations indicate the existence of a possible synergy when they take a higher rank in the list of combinations.

#### **6.4.2. Examining the behaviour of APC-PPP2R1A-X combinations**

CONNECTION OF APC-PPP2CA - Seeling et al. [21] show that PP2A regulatory subunit, B56, interacted with APC in the yeast two-hybrid system and expression of B56 reduced the abundance of  $\beta$ -catenin and inhibited transcription of  $\beta$ -catenin target genes in mammalian cells and Xenopus embryo explants. Further, the B56-dependent decrease in  $\beta$ -catenin was blocked by oncogenic mutations in  $\beta$ -catenin or APC, and by proteasome inhibitors. B56 may direct PP2A to dephosphorylate specific components of the APC-dependent signaling complex and thereby inhibit WNT signaling. Their study suggested that PP2A heterotrimers containing the B56 regulatory subunit functioned in the WNT signaling complex to down-regulate  $\beta$ -catenin, perhaps through an interaction of B56 and the NH<sub>2</sub>-terminus of APC, to dephosphorylate specific components of the APC-dependent signaling complex and thereby inhibit WNT signaling.

Looking at the tables above, one finds the following combinations for APC along with PPP2R1A, to be prominent at 3rd order level - APC-FZD6-PPP2R1A. All these combinations indicate the existence of a possible synergy when they take a higher rank in the list of combinations.

#### **6.4.3. Examining the behaviour of BCL-PPP2R1A-X combinations**

CONNECTION OF BCL-PPP2CA - Deng et al. [22] show that phosphorylation of BCL2 occurs rapidly after the addition of agonist to IL-3-deprived cells and can be reversed by the action of an okadaic acid (OA)-sensitive phosphatase. They make several observations that support the role for PP2A as the BCL2 regulatory phosphatase: • dephosphorylation of BCL2 is blocked by OA, a potent PP1 and PP2A inhibitor; • intracellular PP2A, but not PP1, co-localizes with BCL2; • the purified PP2AC catalytic subunit directly dephosphorylates BCL2 in vitro in an OA-sensitive manner;  $\beta$  the

purified PP2Ac catalytic subunit preferentially dephosphorylates BCL2 in vitro compared with PP1 and PP2B; • reciprocal immunoprecipitation studies indicate a direct interaction between PP2A and hemagglutinin (HA)-BCL2; and • treatment of factor-deprived cells with bryostatin 1 dramatically increases the association between PP2A and BCL2. They propose functional phosphorylation of BCL2 at Ser<sup>70</sup> to be a dynamic process regulated by the sequential action of an agonist-activated BCL2 kinase and PP2A. Via quantitative phospho-proteomic analysis, Brewer et al. [23] identified BCL-9/9L to be substrate of PPP2CA.

Looking at the tables above, one finds the following combinations for members of BCL family along with PPP2R1A, to be prominent at 3rd order level - BCL9-JUN-PPP2R1A, BCL9-FGF4-PPP2R1A and BCL9-PORCN-PPP2R1A. All these combinations indicate the existence of a possible synergy when they take a higher rank in the list of combinations.

#### **6.4.4. Examining the behaviour of Cyclin-PPP2R1A-X combinations**

CONNECTION OF CYCLIN-PPP2CA - Cyclin G2 (CCNG2), together with cyclin G1 (CCNG1) and cyclin I (CCNI), defines a novel cyclin family expressed in terminally differentiated tissues including brain and muscle. Bennin et al. [24] tested the hypothesis that CCNG2 may be a negative regulator of cell cycle progression and found that ectopic expression of CCNG2 induces the formation of aberrant nuclei and cell cycle arrest in HEK293 and Chinese hamster ovary cells. They determined that CCNG2 and its homolog CCNG1 directly interact with the catalytic subunit of PP2A. Further, the ability of CCNG2 to inhibit cell cycle progression correlates with its ability to bind PP2A/B' and C subunits. Together, their findings suggested that CCNG2-PP2A complexes inhibit cell cycle progression.

Looking at the tables above, one finds the following combinations for members of Cyclin family along with PPP2R1A, to be prominent at 3rd order level - CCND2-LRP6-PPP2R1A, CCND3-PPP2R1A-SEN2, CCND1-FGF4-PPP2R1A, CCND1-CTBP1-PPP2R1A, CCND3-PORCN-PPP2R1A and CCND1-JUN-PPP2R1A. All these combinations indicate the existence of a possible synergy when they take a higher rank in the list of combinations.

#### **6.4.5. Examining the behaviour of CSNK-PPP2R1A-X combinations**

CONNECTION OF CSNK-PPP2CA - Casein kinase (CSNK) 1A (CK1A) functions as a pivotal negative regulator of WNT signaling pathway, initiating the events that destabilize  $\beta$ -catenin. Shen et al. [25] show that CK1A activity requires its association with PPP2CA on AXIN, the scaffold protein of the  $\beta$ -catenin destruction complex. They found that WNT stimulation induced the dissociation of PPP2CA from CK1A, which resulted in CK1A autophosphorylation and its consequent inactivation. Further, autophosphorylated CK1A was enriched in a subset of colorectal cancers (CRCs) harboring constitutive WNT activation. Their findings identified a mechanism by which WNT stimulation inactivates CK1A, thus filling a critical gap in understanding of WNT signaling, with relevance for CRC. Via quantitative phospho-proteomic analysis, Brewer et al. [23] identified CSNK-1D/1E/A1 to be substrate of PPP2CA.

Looking at the tables above, one finds the following combinations for members of CSNK family along with PPP2R1A, to be prominent at 3rd order level - CSNK1D-FGF4-PPP2R1A, CSNK2A1-CTBP1-PPP2R1A, CSNK2A1-MYC-PPP2R1A, CSNK2A1-FOXN1-PPP2R1A, CSNK1A1-FGF4-PPP2R1A, CSNK1G1-FGF4-PPP2R1A, CSNK2A1-GSK3A-PPP2R1A, CSNK2A1-NKD1-PPP2R1A, CSNK1G1-FOXN1-PPP2R1A, CSNK1D-PPP2R1A-WNT5A, CSNK1D-PPP2R1A-TCF7L1, CSNK1D-PPP2R1A-TCF7, CSNK2A1-FGF4-PPP2R1A, CSNK1G1-JUN-PPP2R1A, CSNK1G1-PORCN-PPP2R1A, CSNK1D-PORCN-PPP2R1A, CSNK1G1-NLK-PPP2R1A and CSNK1A1-PORCN-PPP2R1A. All these combinations indicate the existence of a possible synergy when they take a higher rank in the list of combinations.

#### **6.4.6. Examining the behaviour of $\beta$ -catenin/CTNNB-PPP2R1A-X combinations**

CONNECTION OF CTNNB(IP)-PPP2CA - Yu et al. [26] show that a heat shock protein HSP105 is required for WNT signaling, since depletion of HSP105 compromises  $\beta$ -catenin concentration and target gene transcription upon WNT stimulation. Mechanistically, they found that HSP105 depletion disrupted the integration of PP2A into the  $\beta$ -catenin degradation complex, thus favoring the hyperphosphorylation and degradation of  $\beta$ -catenin. HSP105 was overexpressed in many types of tumors, thus correlating with increased nuclear  $\beta$ -catenin protein levels and WNT target gene upregulation. Via quantitative phospho-proteomic analysis, Brewer et al. [23] identified CTNNB1 to be substrate of PPP2CA. On the other hand Tago et al. [27] identified a novel catenin beta interacting protein 1 (CTNNBIP1 or ICAT) which inhibited the interaction of  $\beta$ -catenin with TCF-4 and repressed  $\beta$ -catenin/TCF-4-mediated transactivation. Furthermore, ICAT inhibited Xenopus axis formation by interfering with WNT signaling.

Looking at the tables above, one finds the following combinations for members of CTNNB family along with PPP2R1A, to be prominent at 3rd order level - CTNNBIP1-JUN-PPP2R1A, CTNNB1-FOXN1-PPP2R1A, CTNNB1-PORCN-PPP2R1A, CTNNBIP1-FGF4-PPP2R1A, CTNNBIP1-NLK-PPP2R1A and CTNNBIP1-FRAT1-PPP2R1A. All these combinations indicate the existence of a possible synergy when they take a higher rank in the list of combinations.

#### **6.4.7. Examining the behaviour of GSK3-PPP2R1A-X combinations**

CONNECTION OF GSK3-PPP2CA - Hyperphosphorylation of tau is pivotally involved in the pathogenesis of Alzheimer's disease (AD) and related tauopathies. Glycogen synthase kinase-3 $\beta$  (GSK3 $\beta$ ) and PP2A are crucial enzymes to regulate tau phosphorylation. Chu et al. [28] has previously reported the cross-talk between GSK3 $\beta$  and PP2A signaling and showed that PP2A could dephosphorylate GSK3 $\beta$  at Ser9. Chu et al. [28] investigated the dephosphorylation of GSK3 $\beta$  in brain extracts in the presence of phosphatase inhibitors and found that a PP2A-like phosphatase activity was required for dephosphorylation of GSK3 $\beta$  at Ser9. Further, they found that PP2A interacted with GSK3 $\beta$  and suppressed its Ser9 phosphorylation in vitro and in HEK-293FT cells. Activity of PP2A negatively correlated to the level of phosphorylated GSK-3 $\beta$  in kainic acid-induced excitotoxic mouse brain. Via quantitative phospho-proteomic analysis, Brewer et al. [23] identified GSK3-A/B to be substrate of PPP2CA.

Looking at the tables above, one finds the following combinations for members of GSK3 family along with PPP2R1A, to be prominent at 3rd order level - CSNK2A1-GSK3A-PPP2R1A, CTBP1-GSK3A-PPP2R1A, FZD8-GSK3A-PPP2R1A, FRZB-GSK3A-PPP2R1A, DKK1-GSK3A-PPP2R1A, FSHB-GSK3A-PPP2R1A, DAAM1-GSK3A-PPP2R1A, FBXW11-GSK3A-PPP2R1A, DVL1-GSK3A-PPP2R1A, GSK3B-LRP6-PPP2R1A and GSK3B-JUN-PPP2R1A. All these combinations indicate the existence of a possible synergy when they take a higher rank in the list of combinations.

#### **6.4.8. Examining the behaviour of JUN-PPP2R1A-X combinations**

**CONNECTION OF JUN-PPP2CA** - The proto-oncogene c-JUN is a component of activator protein-1 (AP1) transcription factor complexes that regulates processes essential for embryonic development, tissue homeostasis and malignant transformation. Induction of gene expression by c-JUN involves stimulation of its transactivation ability and upregulation of DNA binding capacity. Though it is well known that the c-JUN requires JNK-mediated phosphorylation of S63/S73, the mechanism(s) through which binding of c-JUN to its endogenous target genes is regulated remains poorly characterized. Gilan et al. [29] showed that interaction of c-JUN with chromatin is positively regulated by PP2A complexes targeted to c-JUN by the PR55 $\alpha$  regulatory subunit. PR55 $\alpha$ -PP2A specifically dephosphorylated T239 of c-JUN, thus promoting its binding to genes regulating tumour cell migration and invasion. Their findings suggested a critical role for interplay between JNK and PP2A pathways determining the functional activity of c-JUN/AP1 in tumour cells. Shi et al. [30] indicate that malignant fibrous histiocytoma amplified sequence 1 (MFHAS1) suppresses Toll-like receptor (TLR4) signaling pathway through induction of PP2AC subunit cytoplasm translocation and subsequent c-JUN degradation, leading finally to decrease AP1 activity and cytokines expression. Via quantitative phospho-proteomic analysis, Brewer et al. [23] identified JUN to be substrate of PPP2CA.

Looking at the tables above, one finds the following combinations for JUN along with PPP2R1A, to be prominent at 3rd order level - CTNNBIP1-JUN-PPP2R1A, DKK1-JUN-PPP2R1A, FZD1-JUN-PPP2R1A, FZD8-JUN-PPP2R1A, FOSL1-JUN-PPP2R1A, EP300-JUN-PPP2R1A, BCL9-JUN-PPP2R1A, DVL2-JUN-PPP2R1A, CXXC4-JUN-PPP2R1A, CSNK1G1-JUN-PPP2R1A, FBXW11-JUN-PPP2R1A, FRAT1-JUN-PPP2R1A, CCND1-JUN-PPP2R1A, GSK3B-JUN-PPP2R1A and FZD7-JUN-PPP2R1A. All these combinations indicate the existence of a possible synergy when they take a higher rank in the list of combinations.

#### **6.4.9. Examining the behaviour of FOSL1-PPP2R1A-X combinations**

**CONNECTION OF FOSL1-PPP2CA** - Heterodimerization among the basic-leucine zipper (bZIP) proteins or among the basic-helixloop-helix-leucine zipper (bHLHZip) proteins confers a multitude of combinational activities to these transcription factors. While searching for cellular proteins which could directly interact with bHLHZip protein, USF, Pognonec et al. [31] found a bZIP protein, FRA1/FOSL1. Expression of exogenous USF led to a decrease in AP1-dependent transcription in F9 cells while co-expression of exogenous FRA1/FOSL1 restored the AP1 activity in a dose-dependent

manner.

Further, the nuclear phosphoprotein c-JUN is a major component of the AP1 transcription factor, whose activity is augmented by many oncogenes. An important mechanism to stimulate AP1 function is N-terminal phosphorylation of c-JUN at the serine residues 63 and 73 by the c-JUN N-terminal kinases (JNKs). To determine the function of c-JUN N-terminal phosphorylation (JNP) during oncogenic transformation in vitro and in vivo, Behrens et al. [32] used mice and cells harboring a mutant allele of c-JUN, which has the JNK phosphoacceptor serines changed to alanines (JUN-AA). JUN-AA immortalized fibroblasts expressing v-RAS and v-FOS showed reduced tumorigenicity in nude mice, but the efficiency of v-SRC transformation was unaffected by the lack of JNP. To assess the significance of JNP in tumour development in vivo, two transgenic mouse tumour models were employed. Skin tumour development caused by constitutive activation of the RAS pathway by K5-SOS-F expression and c-FOS-induced osteosarcoma formation were impaired in mice lacking JNP. Thus there is a connection between c-JUN and FOSL1, that might be existing. Finally, figure 4 in Clark and Ohlmeyer [33] shows c-JUN which combines with c-FOS and protein dephosphorylation is initiated by PP2A.

Looking at the tables above, one finds the following combinations for FOSL1 along with PPP2R1A, to be prominent at 3rd order level - CXXC4-FOSL1-PPP2R1A, FOSL1-PPP2R1A-SFRP4, FOSL1-JUN-PPP2R1A, FOSL1-PORCN-PPP2R1A, FOSL1-PPP2R1A-SEN2, FOSL1-PPP2R1A-RHOU and FOSL1-PPP2R1A-TCF7. All these combinations indicate the existence of a possible synergy when they take a higher rank in the list of combinations.

#### **6.4.10. Examining the behaviour of FOX-PPP2CA-X combinations**

CONNECTION OF FOX-PPP2CA - PP2A is a tumour suppressor whose strong inhibition underlies the phosphorylation-dependent, anti-apoptotic mechanisms in chronic lymphocytic leukemia (CLL). Inactivation of PP2A is due to the cooperative action of the phosphorylation of Y307 of its catalytic subunit by the aberrant cytosolic pool of the SRC family kinase LYN and the interaction with its protein inhibitor SET, which is overexpressed in CLL. Pagano et al. [34] developed a library of compounds, the most potent being the one named CC11, which restores PP2A activity by disrupting the PP2A/SET complex, thereby triggering the mitochondrial pathway of apoptosis. They observe that this process involves the recruitment of the proapoptotic BH3-only proteins BAD and BIM to mitochondria, the former upon direct dephosphorylation and the latter being newly expressed upon dephosphorylation and activation of its transcription factor FOXO3A. Their findings highlighted that PP2A antagonized the prosurvival pathways controlled by AKT, which phosphorylates and thereby suppresses a variety of pro-apoptotic factors and tumour suppressors including BAD and FOXO3A.

Looking at the tables above, one finds the following combinations for members of FOX family along with PPP2R1A, to be prominent at 3rd order level - FOXN1-KREMEN1-PPP2R1A, AES-FOXN1-PPP2R1A, CTNNB1-FOXN1-PPP2R1A, DVL1-FOXN1-PPP2R1A, CSNK2A1-FOXN1-PPP2R1A, CSNK1G1-FOXN1-PPP2R1A, FBXW11-FOXN1-PPP2R1A, AXIN1-FOXN1-PPP2R1A, DKK1-FOXN1-PPP2R1A, EP300-FOXN1-PPP2R1A, DAAM1-FOXN1-PPP2R1A and DIXDC1-FOXN1-PPP2R1A. All these



combinations indicate the existence of a possible synergy when they take a higher rank in the list of combinations.

#### **6.4.11. Examining the behaviour of EP300-PPP2R1A-X combinations**

CONNECTION OF EP300-PPP2CA - Transcriptional coactivator p300 (or EP300) is required for embryonic development and cell proliferation. Valproic acid, a histone deacetylase inhibitor, is widely used in the therapy of epilepsy and bipolar disorder. Chen et al. [35] report that valproic acid stimulates proteasome-dependent p300 degradation through augmentation of gene expression of the B56 $\gamma$  regulatory subunits of protein phosphatase 2A. The B56 $\gamma$ 3 regulatory and catalytic subunits of protein phosphatase 2A interact with p300. Overexpression of the B56 $\gamma$ 3 subunit led to proteasome-mediated p300 degradation and repressed p300-dependent transcriptional activation, which required the B56 $\gamma$ 3 interaction domain of p300. Conversely, silencing of the B56 $\gamma$  subunit expression by RNA interference increased the stability and transcriptional activity of p300. Via quantitative phospho-proteomic analysis, Brewer et al. [23] identified EP300 to be substrate of PPP2CA.

Looking at the tables above, one finds the following combinations for EP300 along with PPP2R1A, to be prominent at 3rd order level - EP300-PORCN-PPP2R1A, EP300-FGF4-PPP2R1A, EP300-JUN-PPP2R1A and EP300-FOXN1-PPP2R1A. All these combinations indicate the existence of a possible synergy when they take a higher rank in the list of combinations.

## **7. Conclusion**

This manuscript studies the time behaviour of 3rd order combinations of PPP2R1A in WNT3A stimulated HEK 293 cells. Based on the established 2nd order combinations of the PPP2R1A, 3rd order combinations emerge using the machine learning based search engine. These 3rd order combinations might be of interest for further wet lab investigations.

## **Competing interests**

No competing interest is declared.

## **Author contributions statement**

SS conceived and designed the experiments; wrote the code; performed the experiments; analyzed the data; wrote the manuscript.

## Availability of code

Code for time series data available at CERN based Zenodo on <https://zenodo.org/records/14637456>.

## Acknowledgments

Special thanks to Mrs. Rita Sinha and late Mr. Prabhat Sinha for supporting the author financially, without which this work could not have been made possible.

## Supplementary

The following files (ending with .txt and can be opened in R or in simple text processing program) with these names are made available with this manuscript. For PPP2R1A, (1) **-3-odr-TP-ranking-linear.txt**, (2) **-3-odr-TP-ranking-rbf.txt**, (3) **-3-odr-TP-ranking-2002.txt**, and (4) **-3-odr-TP-ranking-martinez.txt**, contain rankings for 3rd order combinations across each time point for, HSIC (linear kernel), HSIC (rbf kernel), SOBOL (2002 implementation) and SOBOL (martinez implementation), respectively.

## References

- [1] T. S. Gujral, G. MacBeath, A system-wide investigation of the dynamics of wnt signaling reveals novel phases of transcriptional regulation, *PloS one* 5 (2010) e10024.
- [2] S. Sinha, Machine learning ranking of plausible (un) explored synergistic gene combinations using sensitivity indices of time series measurements of wnt signaling pathway, *Integrative Biology* 16 (2024) zya020.
- [3] T. Joachims, Training linear svms in linear time, in: *Proceedings of the 12th ACM SIGKDD international conference on Knowledge discovery and data mining*, ACM, 2006, pp. 217–226.
- [4] P. P. Ruvolo, The broken off switch in cancer signaling: Pp2a as a regulator of tumorigenesis, drug resistance, and immune surveillance, *BBA clinical* 6 (2016) 87–99.
- [5] Y. Shi, Serine/threonine phosphatases: mechanism through structure, *Cell* 139 (2009) 468–484.
- [6] Wikipedia contributors, Protein serine/threonine phosphatase — Wikipedia, the free encyclopedia, [https://en.wikipedia.org/w/index.php?title=Protein\\_serine/threonine\\_phosphatase&oldid=1226576715](https://en.wikipedia.org/w/index.php?title=Protein_serine/threonine_phosphatase&oldid=1226576715), 2024. [Online; accessed 6-March-2025].
- [7] P. Seshacharyulu, P. Pandey, K. Datta, S. K. Batra, Phosphatase: Pp2a structural importance, regulation and its aberrant expression in cancer, *Cancer letters* 335 (2013) 9–18.
- [8] S. Reynhout, V. Janssens, Physiologic functions of pp2a: Lessons from genetically modified mice, *Biochimica Et Biophysica Acta (BBA)-Molecular Cell Research* 1866 (2019) 31–50.
- [9] B. A. Hemmings, C. Adams-Pearson, F. Maurer, P. Muller, J. Goris, W. Merlevede, J. Hofsteenge, S. R. Stone, alpha- and beta-forms of the 65-kda subunit of protein phosphatase 2a have a similar 39 amino acid repeating structure, *Biochemistry* 29 (1990) 3166–3173.
- [10] J. Zhou, H. T. Pham, R. Ruediger, G. Walter, Characterization of the aalpha and abeta subunit isoforms of protein phosphatase 2a: differences in expression, subunit interaction, and evolution, *Biochemical Journal* 369 (2003) 387–398.

- [11] S. Sinha, Hilbert-schmidt and sobol sensitivity indices for static and time series wnt signaling measurements in colorectal cancer-part a, *BMC systems biology* 11 (2017) 120.
- [12] S. Da Veiga, Global sensitivity analysis with dependence measures, *Journal of Statistical Computation and Simulation* 85 (2015) 1283–1305.
- [13] A. Saltelli, Making best use of model evaluations to compute sensitivity indices, *Computer physics communications* 145 (2002) 280–297.
- [14] J. Martinez, Analyse de sensibilité globale par décomposition de la variance, *Presentation in Journée des GdR Ondes & Mascot* 13 (2011) 207.
- [15] M. Baudin, K. Boumhaout, T. Delage, B. Iooss, J.-M. Martinez, Numerical stability of sobol’indices estimation formula, in: *Proceedings of the 8th International Conference on Sensitivity Analysis of Model Output (SAMO 2016)*, volume 30, 2016, pp. 50–51.
- [16] M. Goudreault, L. M. D’Ambrosio, M. J. Kean, M. J. Mullin, B. G. Larsen, A. Sanchez, S. Chaudhry, G. I. Chen, F. Sicheri, A. I. Nesvizhskii, et al., A pp2a phosphatase high density interaction network identifies a novel striatin-interacting phosphatase and kinase complex linked to the cerebral cavernous malformation 3 (ccm3) protein, *Molecular & Cellular Proteomics* 8 (2009) 157–171.
- [17] Y. Xing, Y. Xu, Y. Chen, P. D. Jeffrey, Y. Chao, Z. Lin, Z. Li, S. Strack, J. B. Stock, Y. Shi, Structure of protein phosphatase 2a core enzyme bound to tumor-inducing toxins, *Cell* 127 (2006) 341–353.
- [18] O. Kauko, S. Y. Imanishi, E. Kuleskiy, L. Yetukuri, T. D. Laajala, M. Sharma, K. Pavic, A. Aakula, C. Rupp, M. Jumppanen, et al., Phosphoproteome and drug-response effects mediated by the three protein phosphatase 2a inhibitor proteins cip2a, set, and pme-1, *Journal of Biological Chemistry* 295 (2020) 4194–4211.
- [19] K. Willert, S. Shibamoto, R. Nusse, Wnt-induced dephosphorylation of axin releases  $\beta$ -catenin from the axin complex, *Genes & development* 13 (1999) 1768–1773.
- [20] S. Ikeda, M. Kishida, Y. Matsuura, H. Usui, A. Kikuchi, Gsk-3 $\beta$ -dependent phosphorylation of adenomatous polyposis coli gene product can be modulated by  $\beta$ -catenin and protein phosphatase 2a complexed with axin, *Oncogene* 19 (2000) 537–545.
- [21] J. M. Seeling, J. R. Miller, R. Gil, R. T. Moon, R. White, D. M. Virshup, Regulation of  $\beta$ -catenin signaling by the b56 subunit of protein phosphatase 2a, *Science* 283 (1999) 2089–2091.
- [22] X. Deng, T. Ito, B. Carr, M. Mumby, W. S. May, Reversible phosphorylation of bcl2 following interleukin 3 or bryostatin 1 is mediated by direct interaction with protein phosphatase 2a, *Journal of Biological Chemistry* 273 (1998) 34157–34163.
- [23] A. Brewer, G. Sathe, B. E. Pflug, R. G. Clarke, T. J. Macartney, G. P. Sapkota, Mapping the substrate landscape of protein phosphatase 2a catalytic subunit ppp2ca, *Iscience* 27 (2024).
- [24] D. A. Bennis, A. S. A. Don, T. Brake, J. L. McKenzie, H. Rosenbaum, L. Ortiz, A. A. DePaoli-Roach, M. C. Horne, Cyclin g2 associates with protein phosphatase 2a catalytic and regulatory b’ subunits in active complexes and induces nuclear aberrations and a g1/s phase cell cycle arrest, *Journal of Biological Chemistry* 277 (2002) 27449–27467.
- [25] C. Shen, W. Lu, S. B. Merugu, A. Bharti, S. M. Afify, L. Schnitkey, D. T. Wynn, F. Yang, T. M. Rohwetter, A. Nayak, et al., Wnt signaling inhibits casein kinase 1 $\alpha$  activity by modulating its interaction with protein phosphatase 2a, *Cell Reports* 44 (2025).
- [26] N. Yu, M. Kakunda, V. Pham, J. R. Lill, P. Du, M. Wongchenko, Y. Yan, R. Firestein, X. Huang, Hsp105 recruits protein phosphatase 2a to dephosphorylate  $\beta$ -catenin, *Molecular and cellular biology* 35 (2015) 1390–1400.
- [27] K.-i. Tago, T. Nakamura, M. Nishita, J. Hyodo, S.-i. Nagai, Y. Murata, S. Adachi, S. Ohwada, Y. Morishita, H. Shibuya, et al., Inhibition of wnt signaling by icat, a novel  $\beta$ -catenin-interacting protein, *Genes & development* 14 (2000) 1741–1749.
- [28] D. Chu, J. Tan, S. Xie, N. Jin, X. Yin, C.-X. Gong, K. Iqbal, F. Liu, Gsk-3 $\beta$  is dephosphorylated by pp2a in a leu309 methylation-independent manner, *Journal of Alzheimer’s Disease* 49 (2016) 365–375.

- [29] O. Gilan, J. Diesch, M. Amalia, K. Jastrzebski, A. C. Chueh, N. M. Verrills, R. B. Pearson, J. M. Mariadason, E. Tulchinsky, R. D. Hannan, et al., Pr55 $\alpha$ -containing protein phosphatase 2a complexes promote cancer cell migration and invasion through regulation of ap-1 transcriptional activity, *Oncogene* 34 (2015) 1333–1339.
- [30] Q. Shi, B. Xiong, J. Zhong, H. Wang, D. Ma, C. Miao, Mfhas1 suppresses tlr4 signaling pathway via induction of pp2a c subunit cytoplasm translocation and inhibition of c-jun dephosphorylation at thr239, *Molecular Immunology* 88 (2017) 79–88.
- [31] P. Pognonec, K. E. Boulukos, C. Aperlo, M. Fujimoto, H. Ariga, A. Nomoto, H. Kato, Cross-family interaction between the bhlhzip usf and bzip fra1 proteins results in down-regulation of ap1 activity, *Oncogene* 14 (1997) 2091–2098.
- [32] A. Behrens, W. Jochum, M. Sibilio, E. F. Wagner, Oncogenic transformation by ras and fos is mediated by c-jun n-terminal phosphorylation, *Oncogene* 19 (2000) 2657–2663.
- [33] A. R. Clark, M. Ohlmeyer, Protein phosphatase 2a as a therapeutic target in inflammation and neurodegeneration, *Pharmacology & therapeutics* 201 (2019) 181–201.
- [34] M. A. Pagano, E. Tibaldi, P. Molino, F. Frezzato, V. Trimarco, M. Facco, G. Zagotto, G. Ribaudo, L. Leanza, R. Peruzzo, et al., Mitochondrial apoptosis is induced by alkoxy phenyl-1-propanone derivatives through pp2a-mediated dephosphorylation of bad and foxo3a in cll, *Leukemia* 33 (2019) 1148–1160.
- [35] J. Chen, J. R. St-Germain, Q. Li, B56 regulatory subunit of protein phosphatase 2a mediates valproic acid-induced p300 degradation, *Molecular and cellular biology* 25 (2005) 525–532.